Korean J Physiol Pharmacol
Vol 9: 291–298, October, 2005

Changes of Cytosolic Ca^{2+} under Metabolic Inhibition in Isolated Rat Ventricular Myocytes

Sunghyun Kang*, Nari Kim*, Hyun Joo, Jae Boum Youm, Won Sun Park, Mohamed Warda, Hyungkyu Kim, Dang Van Cuong, Taeho Kim, Euiyong Kim, and Jin Han

Mitochondrial Signaling Laboratory, Department of Physiology and Biophysics, College of Medicine, Cardiovascular & Metabolic Disease Center, Biohealth Products Research Center, Inje University, Busan 614–735, Korea

To characterize cytosolic Ca^{2+} fluctuations under metabolic inhibition, rat ventricular myocytes were exposed to 200 μM 2,4-dinitrophenol (DNP), and mitochondrial Ca^{2+}, mitochondrial membrane potential ($\Delta\Psi_m$), and cytosolic Ca^{2+} were measured, using Rhod-2 AM, TMRE, and Fluo-4 AM fluorescent dyes, respectively, by Laser Scanning Confocal Microscopy (LSCM). Furthermore, the role of sarcolemmal Na^+/Ca^{2+} exchange (NCX) in cytosolic Ca^{2+} efflux was studied in KB-R7943 and Na^+-free normal Tyrode's solution (143 mM LiCl). When DNP was applied to cells loaded with Fluo-4 AM, Fluo-4 AM fluorescence intensity initially increased by 70 ± 10% within 70 ± 10 s, and later by 400 ± 200% at 850 ± 46 s. Fluorescence intensity of both Rhod-2 AM and TMRE were initially decreased by DNP, coincident with the initial increase of Fluo-4 AM fluorescence intensity. When sarcoplasmic reticulum (SR) Ca^{2+} was depleted by 1 μM thapsigargin plus 10 μM ryanodine, the initial increase of Fluo-4 AM fluorescence intensity was unaffected, however, the subsequent progressive increase was abolished. KB-R7943 delayed both the first and the second phases of cytosolic Ca^{2+} overload, while Na^+-free solution accelerated the second. The above results suggest that: 1) the initial rise in cytosolic Ca^{2+} under DNP results from mitochondrial depolarization; 2) the secondary increase is caused by progressive Ca^{2+} release from SR; 3) NCX plays an important role in transient cytosolic Ca^{2+} shifts under metabolic inhibition with DNP.

Key Words: Dinitrophenol, Caffeine, Cytosolic Ca^{2+}, Laser Scanning Confocal Microscopy, Fluo-4 AM, Mitochondria, Ventricular myocytes, NCX, KB-R7943, Rhod-2 AM, TMRE

INTRODUCTION

Intracellular Ca^{2+} plays important roles in the regulation of various cellular functions. They initiate muscle contraction, trigger the release of neurotransmitters from nerve terminals and hormones from secretory cells, regulate gene expression and cell cycle, and mediate cell death. Disrupted Ca^{2+} homeostasis is accompanied by pathological conditions in cells. In particular, ischemia or ischemia/reperfusion injury and cell damage or cell death are associated with extensive cytosolic Ca^{2+} overload (Allshire et al, 1987; Steenbergen et al, 1990). Other authors have shown damage to sarcolemmal structure/function under calcium overload. High cytosolic Ca^{2+} concentrations cause the loss of sarcolemma's ability to bind calcium, leading to calcium deposition in mitochondria. Mitochondrial calcium overload has been considered as an indicator of cell injury (Borgers et al, 1986; Borgers et al, 1987; Ver Donk et al, 1988).

In cardiac myocytes, intracellular Ca^{2+} overload is believed to result from a transient depolarization of the cell membrane, allowing Ca^{2+} entry via the L-type Ca^{2+} channel and leading to limited Ca^{2+} entry (recorded electrically as the L-type Ca^{2+} current (I_{Ca})), followed by triggering of Ca^{2+} release from sarcoplasmic reticulum (SR) (Allan et al, 1994). Sarcolemmal Na^+/Ca^{2+} exchange (NCX), Na^+/H^+ exchange (NHE), L-type calcium channels and K_{ATP} channels play pivotal roles in cytosolic Ca^{2+} regulation under metabolic inhibition (Eisner et al, 1998; Tang et al, 1998; Karmazyn et al, 2001). The present study was undertaken to mimic the events of ischemia or ischemia/reperfusion injury and to characterize the mechanisms of cytosolic Ca^{2+} overload under metabolic inhibition by 2,4-dinitrophenol (DNP). To monitor cytosolic Ca^{2+}, transient fluorescence methods were used with the following: SR NCX reverse mode inhibitor (KB-R7943); SR Ca^{2+} trigger (caffeine); SR Ca^{2+} depletor (thapsigargin/ ryanodine) and NCX inhibitor (Na^+-free Tyrode's solution). Finally, the influence of extracellular Ca^{2+} under DNP was

Corresponding to: Jin Han, Mitochondrial Signaling Laboratory, Department of Physiology and Biophysics, College of Medicine, Cardiovascular and Metabolic Disease Center, Inje University, 633-165 Gaegeum-dong, Busanjin-gu, Busan 614-735, Korea. (Tel) 82-51-890-6714, (Fax) 82-51-894-5714, (E-mail) phyhanj@ijnc.inje.ac.kr
*These two authors contributed equally to this work.

ABBREVIATIONS: DNP, 2,4-dinitrophenol; $\Delta\Psi_m$, mitochondrial inner transmembrane potential; NCX, sarcolemmal Na^+/Ca^{2+} exchange; TMER, tetramethylrhodamine ethyl ester; SR, sarcoplamic reticulum; $[Ca^{2+}]_i$, intracellular CA^{2+} concentration.

examined with Ca^{2+}-free Tyrode's buffer.

Our results indicate that the initial DNP-induced increase of cytosolic Ca^{2+} results from efflux of mitochondrial Ca^{2+} (by depolarization of the mitochondrial inner transmembrane potential ($\Delta\Psi_m$)) and from the influx of extracellular Ca^{2+} into cytosol (via reverse mode sarcolemmal Na^+/Ca^{2+} exchange). Our findings also indicate that the secondary increase of cytosolic Ca^{2+} is due to progressive Ca^{2+} release from SR, and that Na^+/Ca^{2+} exchange (NCX) plays an important role in regulation of cytosolic Ca^{2+} under metabolic inhibition.

METHODS

Isolation of single ventricular cardiomyocytes

Single ventricular myocytes were isolated from rat heart as previously described. Briefly, 8-week-old Sprague-Dawley rats, weighing 280~320 g, were anesthetized by intraperitoneal injection of a mixture of pentobarbital sodium (50 mg/kg body weight) and heparin (300 IU/ml). The heart was rapidly removed by thoracotomy and the aorta was cannulated. The dissected heart was mounted on a Lagendorff apparatus and perfused at 37°C with oxygenated normal Tyrode's for 5~6 min to flush blood from the heart; which was followed by Ca^{2+}-free Tyrode's solution for 5 min, Ca^{2+}-free Tyrode's solution containing 0.01% collagenase (1 mg/10 ml, Yakult) for 25~30 min, and Kraftbruhe (KB) solution for 5~10 min. The heart was then removed from the perfusion apparatus, and the left ventricle was separated by dissection. Single ventricular myocytes were isolated by gentle agitation in KB solution, stored at 4°C, and used within 12 h.

Solutions and drugs

Normal Tyrode's solution contained (mM): 143 NaCl, 5.4 KCl, 1.8 $CaCl_2$, 0.5 $MgCl_2$, 5.5 glucose, and 5 HEPES (pH 7.4) adjusted with KOH. The modified KB solution contained (mM): 25 KCl, 10 KH_2PO_4, 16 KOH, 80 glutamic acid, 10 taurine, 14 oxalic acid, 10 HEPES, and 11 glucose at pH 7.4 adjusted with KOH.

Fluorescent dyes (Fluo-4 AM, Rhod-2 AM, TMRE) were purchased from Molecular Probes (USA), prepared as 1 mM stock solutions in dimethyl sulfoxide (DMSO), and diluted into test solution before each experiment. The final concentration of DMSO was $\leq$0.01%.

The following drugs were used: KB-R7943 or 2-[2-[4-(4-nitrobenzyloxy)phenyl]ethyl]isothiourea methanesulphonate (Oragon), caffeine (Sigma), ryanodine (Sigma), and thapsigargin (Sigma).

Fluorescence measurements

Experiments were performed with a laser scanning confocal microscope (LSM 510 META) coupled to an inverted microscope (Axiovert 200M, Carl Zeiss, Jena, Germany) with a 40x water-immersion objective lens, optimal laser lines and filter. Cells were excited with 514 nm wavelength argon laser, and images were acquired using a >560 nm long-pass filter. Fluorescence of Fluo-4 AM, Rhod-2 AM and TMRE was excited at 488 nm, 560 nm and 564 nm and emitted at 543 nm, 588 nm and 600 nm, respectively. Fluorescence was monitored every 3 s, using time-series image capture. Images were digitized at 8 bits and analyzed using LSM-510 META software (Carl Zeiss, Jena, Germany).

Cytosolic Ca^{2+} and mitochondrial Ca^{2+}

To monitor cytoplasmic Ca^{2+}, the isolated single myocytes were loaded with 3 μM of the acetoxymethyl ester (AM) form of Fluo-4 for 20 min at room temperature. Myocytes were then washed twice by centrifugation (500 rpm, for 5 min each time, in KB solution), and they were transferred into a chamber coated with poly-L-lysine (0.01%) and excited at 488 nm and 560 nm. Emitted light was measured at >580 nm in a confocal microscope.

To monitor mitochondrial Ca^{2+}, myocytes were loaded with mitochondrial Ca^{2+}-sensitive dye, Rhod-2 AM. To adequately load the mitochondria, myocytes were incubated with 5 μM Rhod-2 AM at 4°C for 120 min and for further 20 min at room temperature. After incubation, the cells were washed twice by centrifugation. Rhod-2 AM was excited at 568 nm, and emitted light was measured at >580 nm.

Mitochondrial membrane potential

The cationic dye tetramethylrhodamine ethyl ester, perchlorate (TMRE), was used to monitor time-series changes in mitochondrial membrane potential. Myocytes were incubated with TMRE (200 nM) for 20 min and washed twice by centrifugation. TMRE was excited at 564 nm with helium-neon laser, and emitted signals were collected through a 580 nm long-pass filter. Fluorescence was recorded every 3 s.

Image processing and statistical analysis

Fluorescent images were processed with LSM-510 META software (Carl Zeiss, Jena, Germany), and the imaging systems enabled independent recordings from several cells in the field of view. To represent changes in fluorescence intensity over time, interesting regions of the cells were outlined/highlighted, and the intensity of the chosen region in the image was calculated. In all cases, fluorescence intensity was normalized to the initial value (F_0) recorded in normal Tyrode's solution and compared with the change of intensity as the relative fluorescence (F/F_0).

Data were presented as means$\pm$SEM. Statistical significance was assessed using unpaired t-tests, and $P<0.05$ was considered significant.

RESULTS

DNP induces cytosolic Ca^{2+} overload in two steps

To investigate cytosolic Ca^{2+} overload under metabolic condition inhibited by DNP, rat ventricular myocytes were loaded with Fluo-4 AM and monitored in a confocal microscope after 200 μM DNP was added. Fig. 1A shows that DNP increased Fluo-4 AM fluorescence intensity in two phases: Fluorescence intensity was initially increased by 70$\pm$10% within 70$\pm$10 s (Fig. 1b), and was subsequently increased by 550$\pm$200% within 850$\pm$46 s (Fig. 1d). Cell shortening began after 600$\pm$16 s and reached rigor contraction after 646$\pm$77 s (Fig. 1c).

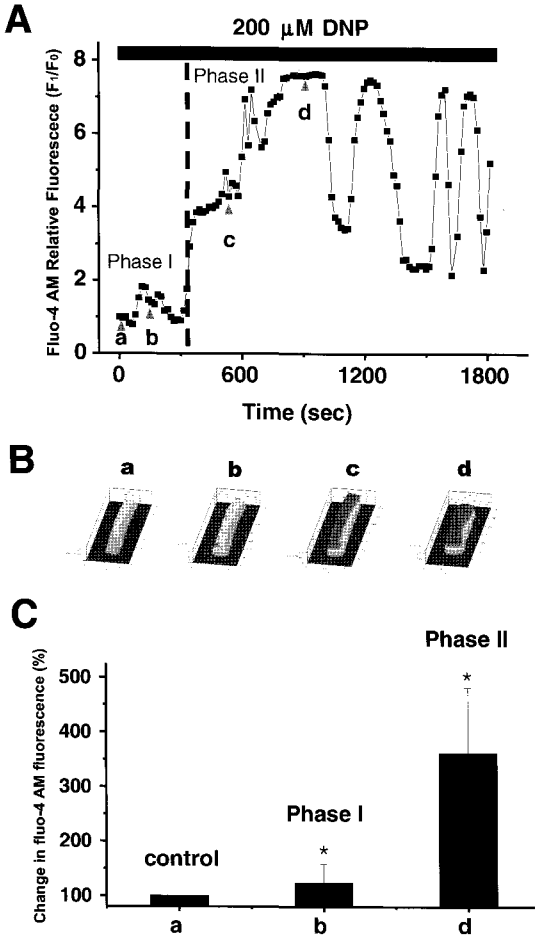

Fig. 1. The effect of DNP on cytosolic Ca^{2+} in an isolated rat ventricular myocyte. (A) Record of Fluo-4 AM fluorescence from a single myocyte loaded with 4 mM Fluo-4 AM under 200 μM DNP in confocal microscopy. DNP was applied as indicated by the bar. (B) The confocal image of control, a; phase I, b; beginning of contraction, c; peak point of phase II in the cell. (C) Mean increase of Fluo-4 AM fluorescence during phase I and phase II from 6 cells. Phase I and phase II fluorescence were seen at about 30 s (a) and 300 s (b), and increased by about 50% (b) and 400% (d), respectively, after DNP application. *$P<0.05$ compared to pre-DNP value (control, a).

DNP causes mitochondrial depolarization and an initial increase of cytosolic Ca^{2+}

DNP is a protonophore that can reduce the potential across inner mitochondrial membrane, and mitochondrial depolarization could possibly release mitochondrial Ca^{2+} into cytosol. To investigate the role of mitochondrial Ca^{2+} in cytosolic Ca^{2+} overload under DNP, isolated myocytes were loaded with a mitochondrial membrane potential-sensitive dye (TMRE) and with Fluo-4 AM: Positively-charged TMRE accumulates in the mitochondrial membrane, which carries a high negative charge, and mitochondrial depolarization causes a loss of TMRE intensity. Fig. 2A and B shows that Fluo-4 AM fluorescence (SQR) was increased by 30±5% after 300 s, while TMRE fluorescence (CIR) was decreased by 90±10%, corresponding to mitochondrial depolarization and the rise of cytosolic Ca^{2+} after DNP exposure. Similarly, the mitochondrial Ca^{2+}-sensitive fluorescent dye, Rhod-2 AM, was used to examine mitochondrial Ca^{2+} release, and Fig. 2D and E show that Rhod-2 AM fluorescence (SQR) was decreased by 30±7% within 100 s, remained low until 300 s, thereafter, increased during 330 s and 800 s. This also showed that the decrease in mitochondrial Ca^{2+} coincided with mitochondrial depolarization and with the initial rise in cytosolic Ca^{2+} under DNP. These results suggest that DNP causes the initial overload of cytosolic Ca^{2+} by mitochondrial depolarization.

Depletion of sarcoplasmic reticulum Ca^{2+} abolishes the secondary rise in cytosolic Ca^{2+}

To investigate the role of sarcoplasmic reticulum (SR) in DNP-induced cytosolic Ca^{2+} overload, cells loaded with Fluo-4 AM were superfused for 10 min with Ca^{2+}-free Tyrode's solution containing ryanodine (10 μM) and thapsigargin (1 μM) to block the effect of SR Ca^{2+}. After ryanodine/thapsigargin pretreatment, cells were perfused with normal Tyrode's solution containing DNP (200 μM). Fig. 3A and B shows that fluorescence was initially increased by 10±7% within 300 s and decreased by 10±5% after 300 s. These results indicate that the secondary rise of cytosolic Ca^{2+} under DNP is due to release of SR Ca^{2+}.

Cytosolic Ca^{2+} fluctuations during metabolic inhibition by DNP

To probe the regulation of cytosolic Ca^{2+} under metabolic inhibition by DNP, caffeine (10 mM) and DNP were added to the cells loaded with Fluo-4 AM. Continuous perfusion with caffeine caused cytosolic Ca^{2+} overload via SR Ca^{2+} release and inhibition of Ca^{2+} reuptake by SR. Cells were continuously perfused with normal Tyrode's containing caffeine, either without (Fig. 4A) or with (Fig. 4D) DNP. Fluorescence was increased by 180±20% (Fig. 4A, B) after application of DNP and caffeine. After cytosolic Ca^{2+} overload, fluorescence was decreased by 40±10% (Fig. 4A, B) and 50±7% (Fig. 4D, E), respectively, within 1,200 s. Cytosolic Ca^{2+} fluctuation is shown in Fig. 4D. These results suggest that metabolic inhibition under DNP inhibits cytosolic Ca^{2+} efflux, possibly by inhibiting of reverse phase NCX or other mechanisms.

Sarcolemmal Na^{+}/Ca^{2+} exchange regulates cytosolic Ca^{2+} overload under DNP

To investigate the role of sarcolemmal Na^{+}/Ca^{2+} exchange (NCX) under metabolic inhibition by DNP, an inhibitor of reverse mode NCX (KB-R7943) or Na^{+}-free Tyrode's solution (143 mM LiCl) was applied to myocytes loaded with Fluo-4 AM. Before DNP application in normal Tyrode's solution, cells were superfused for 10 min with either normal Tyrode's solution that contained KB-R7943 (10 mM) or with Na^{+}-free Tyrode's solution (143 mM LiCl). Figure 5A shows that, under DNP, KB-R7943 delayed phases I and II of cytosolic Ca^{2+} overload by 2000±100 s and 3000±200 s, respectively. However, Fig. 5B shows that pretreatment with Na^{+}-free Tyrode's solution accelerated phase II of cytosolic Ca^{2+} overload under DNP by 50±10 s. This suggests that reverse mode NCX causes the initial overload of cytosolic Ca^{2+} and triggers Ca^{2+} release from SR under metabolic inhibition by DNP.

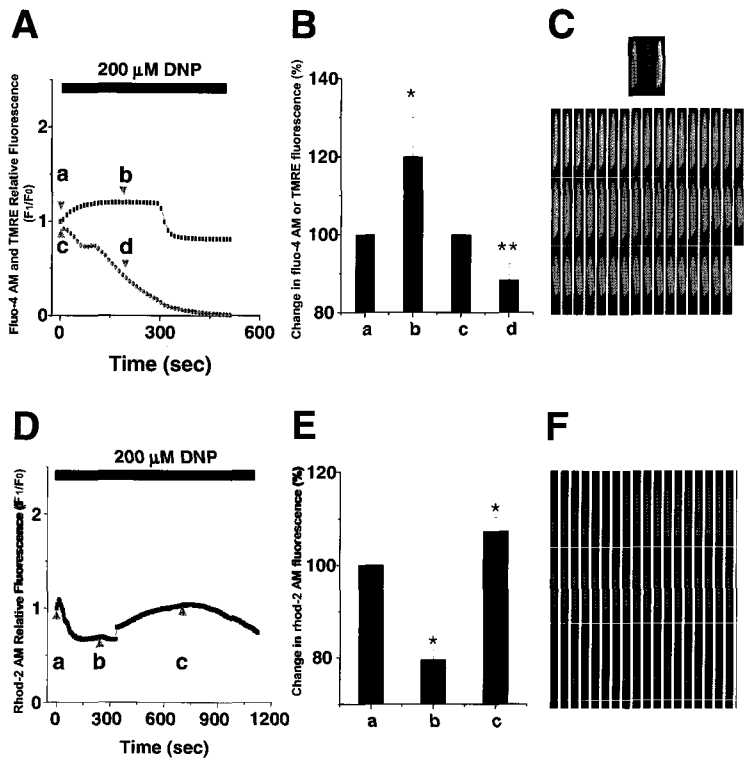

Fig. 2. The role of mitochondria on the rise of cytosolic Ca^{2+} after DNP. Cells were loaded with both 3 μM Fluo-4 AM (SQR) and 200 nM TMRE (CIR) (A, B, C) or with 4 μM Rhod-2 AM (SQR) (D, E, F). Fluorescence changes in the presence of DNP were monitored by confocal microscopy. (A) Record of fluorescence changes in a myocyte loaded with both Fluo-4 AM and TMRE under DNP. (B) Mean fluorescence change in both Fluo-4 AM and TMRE during phase I (a: control of Fluo-4 AM fluorescence, b: phase I of Fluo-4 AM fluorescence was increased by 30%, $*P<0.05$ vs a, c: control of TMRE fluorescence, d: phase 1 of TMRE fluorescence), $**P<0.05$ vs c. (C) Confocal image of Fluo-4 AM and TMRE. (D) Record of Rhod-2 AM fluorescence. (E) Mean change of Rhod-2 AM fluorescence after DNP application in confocal microscopy (a: control of Rhod-2 AM, b: phase 1 of Rhod-2 AM fluorescence was decreased by 30%, $*P<0.05$ vs a, c: phase 2 of Rhod-2 AM fluorescence change). (F) Confocal image of Rhod-2 AM loaded myocytes.

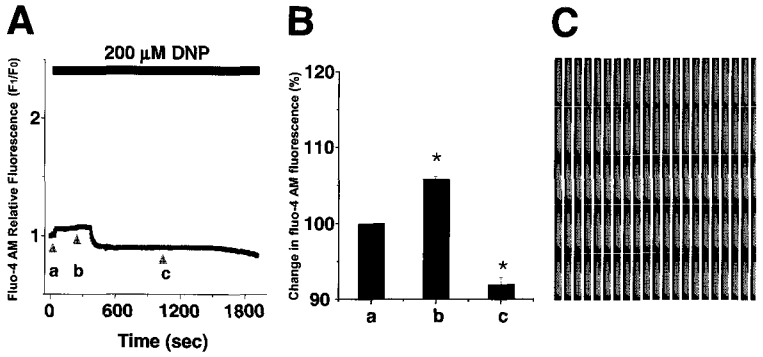

Fig. 3. SR Ca^{2+} depletion abolishes the phase II cytosolic Ca^{2+} rise under DNP. (A) After SR Ca^{2+} depletion by pretreatment with 10 μM ryanodine and 1 μM thapsigargin, Fluo-4 AM fluorescence under DNP was recorded in a single myocyte loaded with Fluo-4 AM. (B) Mean change of Fluo-4 AM fluorescence (a: control, b: Fluo-4 AM fluorescence change during phase I, c: Mean fluorescence change in phase II) ($*P<0.05$ vs a: control).

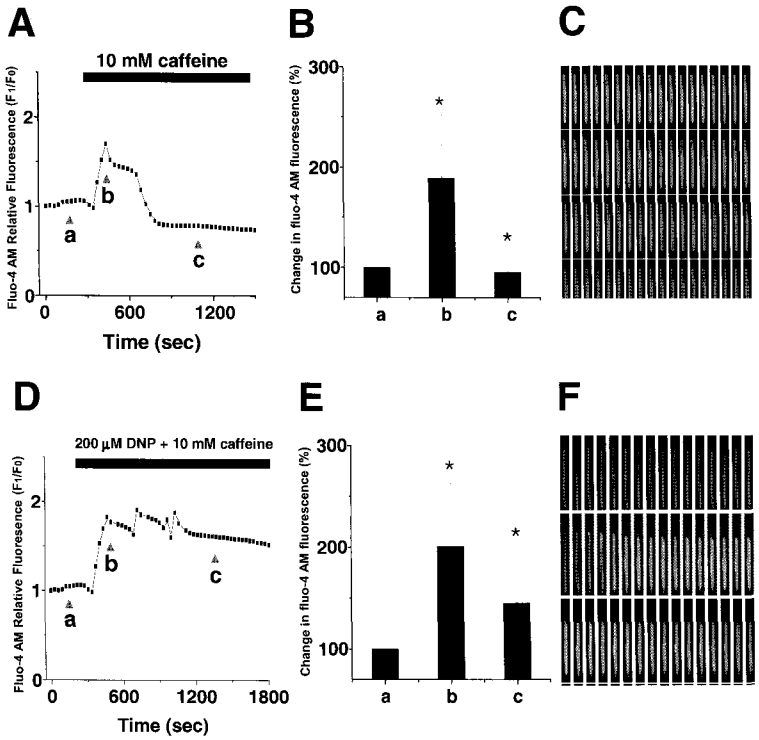

Fig. 4. Cytosolic Ca^{2+} removal after SR Ca^{2+} release by 10 mM caffeine in the absence of DNP (A: fluorescence recording, B: summarized data, C: confocal image) or in the presence of DNP (D: fluorescence recording, E: summarized data, F: confocal image). (A) Record of Fluo-4 AM fluorescence from a single myocyte loaded with Fluo-4 AM (a: control, b: increased fluorescence with caffeine, c: the removed fluorescence) in confocal microscopy. (B) Fluorescence of Fluo-4 AM increased by 100% (Bb, Eb), and, in the absence and presence of DNP, the increase of fluorescence was reduced by about 100% and 50%, respectively. $^*P<0.05$ vs control.

Extracellular Ca^{2+} affects secondary cytosolic Ca^{2+} overload under DNP

To examine the effect of extracellular Ca^{2+} on the rise of cytosolic Ca^{2+} under DNP, the myocytes loaded with Fluo-4 AM were superfused for 3 min with Ca^{2+}-free Tyrode's solution, and were then exposed to DNP. Figure 5C shows that fluorescence intensity initially fluctuated slightly within 20±5%, until 2400 s. And, following an abrupt increase of 450±100%, fluorescence intensity decreased to baseline at 3200 s. These findings indicate that extracellular Ca^{2+} also plays a role in the initial Ca^{2+} overload under DNP.

DISCUSSION

In this study, we investigated the mechanisms of cytosolic Ca^{2+} overload under metabolic condition inhibited by DNP. Our results show that DNP caused a two-phase increase of cytosolic Ca^{2+} in isolated rat ventricular myocytes. DNP caused an initial cytosolic Ca^{2+} overload, seen as an increase of about 30% in the fluorescence intensity of Fluo-4 AM (a cytosolic Ca^{2+}-specific fluorescent dye), which was followed later by a greater increase of cytosolic Ca^{2+}. Fluo-4 AM and a mitochondrial Ca^{2+}-specific fluorescent dye (Rhod-2 AM) were used to examine these rises of cytosolic Ca^{2+}. The initial increase of Fluo-4 AM fluorescence intensity under DNP coincided with the loss of Rhod-2 AM fluorescence intensity. To investigate the correlation between the mitochondrial inner transmembrane potential ($\Delta\Psi_m$) and cytosolic Ca^{2+} under metabolic inhibition, myocytes were loaded simultaneously with TMRE and Fluo-4 AM, and then exposed to DNP. DNP caused a loss of TMRE fluorescence intensity, which coincided with increased intracellular Fluo-4 AM fluorescence intensity. These findings suggest that DNP can cause efflux of mitochondrial Ca^{2+} into the cytosol by depolarization of the $\Delta\Psi_m$, coincident with an increase of cytosolic Ca^{2+}. Montero et al (2001) recently demonstrated that when $\Delta\Psi_m$ was depolarized, the Ca^{2+} uniporter functions in reverse and releases mitochondrial Ca^{2+} into the cytosol.

Opening and closing of the mitochondrial permeability transition pore (mPTP) are regulated by multiple factors such as reactive oxygen radicals, and matrix pH, $[Ca^{2+}]_m$, and $\Delta\Psi_m$. mPTP opening allow nonselective ion permeability of a mitochondrial Ca^{2+} flux that depends on the gradient of Ca^{2+} concentration between the cytosplasm and the mitochondria. It should be noted, however, that the nonselective pore could leak the fluorescent probe from the mitochondria (Crompton et al, 1999; Halestrap et al, 2000; Masao et al, 2005).

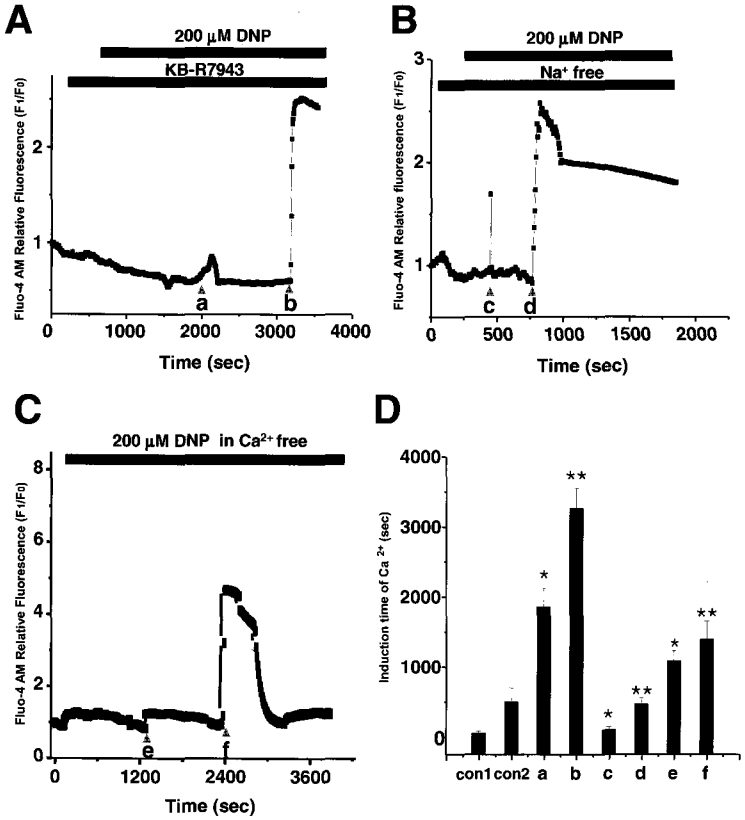

Fig. 5. The role of sarcolemmal NCX in cytosolic Ca^{2+} efflux. Fluo-4 AM loaded cells were treated with sarcolemmal NCX inhibitor, (A) 10 mM KB-R7943 and (B) Na^{+}-free Tyrode's, respectively, and (C) Ca^{2+}-free Tyrode's before and during DNP addition. (D) Summarized data of Ca^{2+} overload (phase 1, phase 2) was monitored using Fluo-4 AM (con1 and con2 indicate b and d, respectively in Fig. 1, a: phase 1 of A, b: phase 2 of A, c: phase 1 of B, d: phase 2 of B, e: phase 1 of C, f: phase 2 of C). $^{*}P<0.05$ compared to con1 and $^{**}P<0.05$ vs con2.

During ischemia, anaerobic glycolysis and ATP degradation induce H^{+} that activate the Na^{+}/H^{+} (Cross HR et al, 1996). Exchanger (NHE) causes Na^{+} influx, because the Na^{+}/K^{+} ATPase is inhibited under ischemia (Cross HR et al, 1995), and Na^{+} efflux decreases, leading to intracellular Na^{+} rise. This intracellular Na^{+} rise under ischemia is accompanied by cytosolic Ca^{2+} overload (Weiss RG et al, 1990; Murphy E et al, 1991).

Mitochondrial NCX (mitoNCX) is also a well known primary pathway of Ca^{2+} efflux in cardiomyocytes. Even though mitoNCX activity is impaired when $\Delta\Psi_m$ is dissipated, mitoNCX effluxes mitochondrial Ca^{2+} into cytosol even after $\Delta\Psi_m$ dissipation (Saotome et al, 2005). We also investigated the role of extracellular Ca^{2+} and sarcolemmal NCX in the initial increase of cytosolic Ca^{2+} under DNP. When DNP was applied, to cells loaded with Fluo-4 AM in the absence of extracellular Ca^{2+}, both the initial and the secondary Ca^{2+} overload were delayed by 1800 s: Cytosolic Ca^{2+} overload under DNP was more accelerated and delayed, respectively, when myocytes loaded with Fluo-4 AM were challenged with Na^{+} free Tyrode's solution and the reverse mode sarcolemmal NCX inhibitor, KB-R7943. Therefore, we postulate that extracellular Ca^{2+} and reverse mode sarcolemmal NCX are involved in the first and the second phases of cytosolic Ca^{2+} overload under DNP. KB-R7943 potently inhibits NCX-mediated Ca^{2+} overload and membrane currents in cardiac myocytes and that the EC_{50} for the inhibition of reverse mode of NCX was 3~10 μM (Iwamoto et al, 2001).

In contrast, Hudman et al (2002) found that both the first and the second phases of cytosolic Ca^{2+} overload under DNP were uninfluenced by extracellular Ca^{2+}. Furthermore, an active form of DNP has been known as K^{+} channel opening drugs, inducing K_{ATP} channel via not only pH (Forestier et al, 1994; Decking et al, 1995; Terzic et al, 1995), but also ATP-dependent mechanisms. DNP-induced opening of K_{ATP} channels was associated with suppression of Na^{+} and Ca^{2+} current, which is known to be sensitive to metabolic stress (Terzic et al, 1994B).

The second phase of cytosolic Ca^{2+} overload was investigated by abolishing SR with thapsigargin plus ryanodine. In this case, the initial increase of cytosolic Ca^{2+} was still seen, but the secondary increase disappeared. This suggests that the second phase was caused by release of Ca^{2+} from the SR. Subsequent work showed that the subcellular mechanism for Ca^{2+}-induced release of calcium (CICR) was a Ca^{2+}-dependent opening probability of the SR Ca^{2+} release (Rousseau et al, 1986). L-type Ca^{2+} channel and sarcolemmal NCX trigger for SR Ca^{2+} release (Levi et al, 1993; Kohmoto et al, 1994; Eisner et al, 1998).

In particular, an increase of local Na^+ concentration initiates Ca^{2+} entry via Na^+/Ca^{2+} exchange, and depolarization may lead directly to Ca^{2+} entry via the exchange (Leblanc et al, 1990).

Sarcolemmal depolarization is thought to produce a conformational change in the dihydropyridine receptor and to induce the release of Ca^{2+} from the SR (Rios & Piaxarro, 1991; Rios et al, 1993; Schneider, 1994). Chronic inhibition of the L-type calcium channel, but not of the T-type channel, may enhance the Ca^{2+} release mediated by the ryanodine receptor. This may explain the development of tolerance to the inhibitory effects on K^+-induced increases in $[Ca^{2+}]_i$ caused by nifedipine and verapamil (Czarnowska et al, 1998). Recently, it has been shown that mitochondrial membrane potential enhances Ca^{2+} entry into mitochondrial matrix via Ca^{2+} uniporter, thereafter, depolarization of mitochondrial membrane potential cause increase of cytosolic Ca^{2+} (Delcamp TJ et al, 1998).

Even though DNP is used as a metabolic inhibitor, it has been administered as a preconditioning factor for cardiac ischemia, similar to cyclosporin A, adenosine, and trimetazidine. K_{ATP} channel openers increase cell viability and protect cells by reducing mitochondrial Ca^{2+} under conditions such as ischemia, ischemia/reperfusion or hypoxia/reoxygenation (Veitch et al, 1995; Elimadi et al, 1997; Holmuhamedov et al, 1998; Minners et al, 2000).

In summary, these studies suggest that: 1) reverse mode sarcolemmal Na^+/Ca^{2+} exchange and extracellular Ca^{2+} are associated with the first phase of cytosolic Ca^{2+} overload under DNP, and 2) DNP also causes mitochondrial Ca^{2+} efflux into the cytosol by depolarizing the $\Delta\Psi_m$. This first phase of cytosolic Ca^{2+} overload might trigger SR Ca^{2+} release and elicit the second phase.

ACKNOWLEDGEMENT

This work was supported by Korea Research Foundation Grant funded by Korea Government (KRF-2005-210-E00003, KRF-2005-211-E00006, KRF-2003-015-E00025, KRF-2002-042-E00006) and the Research Project on the Production of Bio-organs, Ministry of Agriculture and Forestry, Republic of Korea.

REFERENCES

Allshire A, Piper HM, Cuthbertson KSR, Cobbold PH. Cytosolic free Ca^{2+} in single rat heart cells during anoxia and reoxygenation. *Biochem J* 244: 381–385, 1987

Borgers M, Shu LG, Xhonneux B, Thone F, Van Overloop P. Changes in ultrastructure and Ca^{2+} distribution in the isolated working rabbit heart after ischemia. A time related study. *Am J Pathol* 126: 92–102, 1987

Borgers M, Thone F, Verheyen A, Ter Keurs HE. Localization of calcium in skeletal and cardiac muscle. *Histochem J* 16: 295–309, 1984

Borgers M, Piper HM Calcium shifts in anoxic cardiac myocytes. A cytochemical study. *J Mol Cell Cardiol* 18: 439–448, 1986

Cross HR, Opie LH, Radda GK, Clarke K. Is high glycogen beneficial or detrimental to the ischaemic rat heart? A controversy resolved. *Circ Res* 78: 482–491, 1996

Cross HR, Radda GK, Clarke K. The role of Na11/K1 ATPase activity during low flow ischemia in preventing myocardial injury: A 31P, 23Na1 and 87Rb NMR spectroscopic study. *Magn Reson Med* 34: 673–685, 1995

Czarnowska E, Karwatowska-Prokopczuk E, Kurzydlowski K. Ultrastructural study of calcium shift in ischemic/reperfused rat heart under treatment with dimethylthiourea, diltiazem and amiloride. *Basic Res Cardiol* 93: 269–275, 1998

Decking UK, Reffelmann T, Schrader J, Kammermeier H. Hypoxia-induced activation of KATP channels limits energy depletion in the guinea pig heart. *Am J Physiol* 269: H734–H742, 1995

Delcamp TJ, Dales C, Ralenkotter L, Cole PS, Hadley RW. Intramitochondrial $[Ca^{2+}]$ and membrane potential in ventricular myocytes exposed to anoxia-reoxygenation. *Am J Physiol* 275: H484–H494, 1998

Hudman D, Rinbow RD, Lawrence CL, Standen NB. The origin of calcium overload in rat cardiac myocytes following metabolic inhibition with 2,4-Dinitrophenol. *J Mol cell cardiol* 34: 859-871, 2002

Eisner DA, Trafford AW, Diaz ME, Overend CL, O'Neill SC. The control of Ca release from the cardiac sarcoplasmic reticulum: regulation versus autoregulation. *Cardiovasc Res* 38: 589–604, 1998

Elimadi A, Morin D, Sapena R, Chauvet-Monges AM, Crevat A, Tillement JP. Comparison of the effects of cyclosporine A and trimetazidine on Ca -dependent mitochondrial swelling. *Fundam Clin Pharmacol* 11: 440–447, 1997

Forestier C, Pierrard J, Vivaudou M. Mechanism of action of K-Channel-Openers on skeletal muscle KATP channels: Interaction with nucleotides and protons. *J. Gen. Physiol.* 107: 489–502, 1996

Haigney MC, Miyata H, Lakatta EG, Stern MD, Silverman HS. Dependence of hypoxic cellular calcium loading on Na^+-Ca^{2+} exchange. *Circ Res* 71: 547–557, 1992

Holmuhamedov EL, Jovanovic S, Dzeja PP, Jovanovic A, Terzic A. 1 Mitochondrial ATP-sensitive K channels modulate cardiac mitochondrial function. *Am J Physiol* 275: H1567–1576, 1998

Iwamoto T, Kita S, Uehara A, Inoue Y, Taniguchi Y, Imanaga I. and Shigekawa, M. Structural domains influencing sensitivity to isothiourea derivative inhibitor KB-R7943 in cardiac Na^+/Ca^{2+} exchanger. *Mol Pharmacol* 59: 524–531, 2001

Karmazyn M, Sostaric JV, Gan XT. The myocardial Na^+/H^+ exchanger: a potential therapeutic target for the prevention of myocardial ischaemic and reperfusion injury and attenuation of postinfarction heart failure. *Drugs* 61: 375–389, 2001

Kohmoto O, Levi AJ, Bridge JHB. Relation between reverse sodium-calcium exchange and sarcoplasmic reticulum calcium release in guinea pig ventricular cells. Circ Res 74: 550–554, 1994

Levi AJ, Brooksby P, Hancox JC. A role for depolarisation induced calcium entry on the Na-Ca exchange in triggering intracellular calcium release and contraction in rat ventricular myocytes. *Cardiovasc Res* 27: 1677–1690, 1993

Minners J, van den Bos EJ, Yellon DM, Schwalb H, Opie LH, Sack MN. Dinitrophenol, cyclosporin A, and trimetazidine modulate preconditioning in the isolated rat heart: support for a mitochondrial role in cardioprotection. *Cardiovasc Res* 47: 68–73, 2000

Murphy E, Perlman M, London RE, Steenbergen C. Amiloride delays the ischemic-induced rise in cytosolic free calcium. *Circ Res* 68: 1250–1258, 1991

Rios E, Karhanek M, Ma J. An allosteric model of the molecular interactions of excitation-contraction coupling in skeletal muscle. *J Gen Physiol* 102: 449–481, 1993

Rios E, Pizarro G. Voltage sensor of excitation-contraction coupling in skeletal muscle. *Physiol Rev* 71: 849–908, 1991

Rousseau E, Smith JS, Henderson JS, Meissner G. Single channel and $^{45}Ca^{2+}$ flux measurements of cardiac sarcoplasmic reticulum calcium channel. *Biophys J* 50: 1009–1014, 1986

Saotome M, Katoh H, Satoh H, Nagasaka S, Yoshihara S, Terada H, Hayashi H. Mitochondrial membrane potential modulates regulation of mitochondrial Ca^{2+} in rat ventricular myocytes. *Am J Physiol Heart Circ Physiol* 288: H1820–H1828, 2005

Schneider MF. Control of calcium release in functioning skeletal muscle fibers. *Annu Rev Physiol* 56: 463–484, 1994

Steenbergen C, Murphy E, Watts JA, London RE Correlation between cytosolic free calcium, contracture, ATP and irreversible ischaemic injury in perfused rat heart. *Circ Res* 66: 135−146, 1990

Tang T, Duffield R, Ho AK. Effects of Ca^{2+} channel blockers on Ca^{2+} loading induced by metabolic inhibition and hyperkalemia in cardiomyocytes. *Eur J Pharmacol* 360: 205−211, 1998

Terzic A, Jahangir A, Kurachi Y. HOE-234, a second generation K^+ channel opener, antagonizes the ATP-dependent gating of cardiac ATP-sensitive K^+ channels. *J Pharmacol Exper Ther* 68: 818−825, 1994b

Terzic A, Jahangir A, Kurachi Y. Cardiac ATP-sensitive K^+ channels: regulation by intracellular nucleotides and K^+ channelopening drugs. *Am J Physiol* 269: C525−C545, 1995

Veitch K, Maisin L, Hue L. Trimetazidine effects on the damage to mitochondrial functions caused by ischemia and reperfusion. *Am J Cardiol* 76: 25B−30B, 1995

Ver Donck L, Van Reempts J, Vandeplassche G, Borgers M. A new method to study activated oxygen species induced damage in cardiomyocytes and protection by Ca^{2+}-antagonists. *J Mol Cell Cardiol* 20: 811−823, 1988

Wasserstrom JA, Vites AM. The role of Na^+-Ca^{2+} exchange in activation of excitation-contraction coupling in rat ventricular myocytes. *J Physiol London* 493: 529−542, 1997

Weiss RG, Lakatta EG, Gerstenblith G. Effects of amiloride on metabolism and contractility during reoxygenation in perfused rat hearts. *Circ Res* 66: 1012−1022, 1990